Passively mode-locked fiber laser based on a hollow-core photonic crystal fiber filled with few-layered graphene oxide solution

Zhi-Bo Liu,[1,2] Xiaoying He,[1] and D. N. Wang[1,*]

[1]*Department of Electrical Engineering, The Hong Kong Polytechnic University, Hung Hom, Kowloon, Hong Kong*

[2]*Key Laboratory of Weak Light Nonlinear Photonics, Ministry of Education, Teda Applied Physics School, Nankai University, Tianjin 300457, China*

**Corresponding author: eednwang@polyu.edu.hk*

Received May 26, 2011; accepted July 1, 2011;
posted July 6, 2011 (Doc. ID 148270); published August 4, 2011

We demonstrate a nanosecond-pulse erbium-doped fiber laser that is passively mode locked by a hollow-core photonic crystal fiber filled with few-layered graphene oxide solution. Owing to the good solution processing capability of few-layered graphene oxide, which can be filled into the core of a hollow-core photonic crystal fiber through a selective hole filling process, a graphene saturable absorber can be successfully fabricated. The output pulses obtained have a center wavelength, pulse width, and repetition rate of 1561.2 nm, 4.85 ns, and 7.68 MHz, respectively. This method provides a simple and efficient approach to integrate the graphene into the optical fiber system.

OCIS codes: 140.3510, 160.4236.

Passively mode-locked erbium-doped fiber lasers have many applications ranging from basic research to telecommunications, medicine, and materials processing because of their simple and compact design and high-quality pulse generation. A saturable absorber (SA) is usually used as the mode-locking technique to turn the laser continuous wave into a train of short optical pulses. Semiconductor SA mirrors always dominate passive mode locking in spite of their complex fabrication and narrow tuning range [1,2]. Recently, two simple and cost-effective alternatives, single walled carbon nanotubes (SWCNTs) and graphene, have also attracted considerable attention. Both SWCNTs and graphene have advantages, such as ultrafast recovery time, large saturable absorption, ease of fabrication, and low cost. Using a mode-locking technique, optical pulses from sub 200 femtoseconds to a few nanoseconds have been reported for SWCNT-based SAs and graphene-based SAs [3–17]. However, graphene may be superior to SWCNTs in broadband mode-locking due to its gapless linear dispersion of Dirac electrons [18].

Graphene—polymer composites [17], chemical vapor deposition-grown films [12], functionalized graphene [10], and reduced graphene oxide (GO) flakes [14] have been used for ultrafast lasers. The common method of integrating graphene SAs in laser cavities is to sandwich a graphene SA film between two fiber connectors with a fiber adaptor [10–13,15–17]. However, it is known that solubility and/or processability are the first issues for many prospective applications of graphene-based materials [19]. Although GO has a good solubility in water and many organic solvents, unfortunately carbon atoms bonded with oxygen groups are sp^3 hybridized and disrupt the sp^2 conjugation of the hexagonal graphene lattice in GO and thus destroy the linear dispersion of the Dirac electrons and influence the unique optical properties of graphene [20]. This makes GO unsuitable as a broadband SA in laser cavities for ultrafast pulse generation. Thus, a solution-phase graphene with large SA becomes crucially important because it can easily be integrated into a range of photonic systems. Furthermore, a solution-phase graphene can provide a robust method of nonlinear interaction of the guided mode, which has the potential benefit of increasing the damage threshold of the SA for high power pulse formation in laser cavity.

Here, using a selective hole filling technique, we report an erbium-doped fiber laser mode locked by a hollow-core photonic crystal fiber (HC-PCF) filled with few-layered graphene oxide (FGO) solution. The good solution processing capability of FGO makes it possible to be filled into the core of HC-PCF. The cavity comprises sections with normal and anomalous dispersion and the output pulses of 4.85 ns are obtained at the center wavelength of 1561.2 nm.

Our all-fiber mode-locked ring laser setup is shown in Fig. 1. A 1.5 m heavily erbium-doped fiber (OFS EDF-80) is used as the gain medium, pumped by a 1480 nm high power laser diode through a wavelength division multiplexer coupler. A polarization controller (PC) is used to optimize the mode-locking operation while a polarization independent isolator maintains the unidirectional

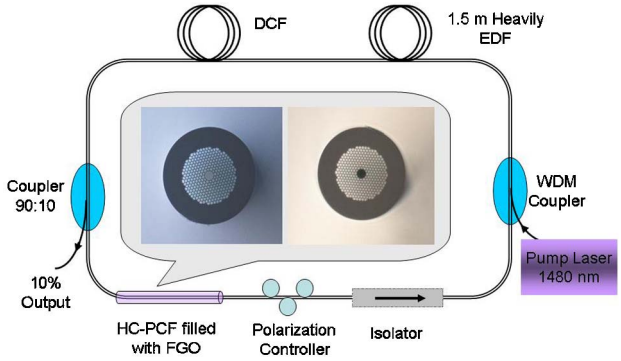

Fig. 1. (Color online) Experimental setup for fiber pulsed laser with HC-PCF filled with FGO solution. Insets are the cross section images of the HC-PCF before (right) and after (left) infiltration of FGO solution.

laser pulse propagation. The mode-locked pulses can be directed out by use of a 90:10 coupler. The group velocity dispersion (GVD) is one of the key factors to maintain the fiber laser operation stability. The GVD of the dispersion compensation fiber used in the system is ~ -30.5 ps/nm/km and that of the EDF is ~ -46.25 ps/nm/km, at the wavelength of 1560 nm. The whole cavity length is about 27.1 m. The rest of the cavity consists of single mode fiber (SMF), which has anomalous dispersion at 1560 nm, with GVD of ~28 ps/nm/km. The HC-PCF filled with FGO solution is 12 cm in length and has a large normal dispersion of ~ -186 ps/nm/km. Thus, the total intracavity dispersion obtained is ~0.53 ps^2, typical of a dispersion-managed fiber laser cavity [21]. Two sections of SMF of 50 cm in length were spliced to the HC-PCF filled with FGO using a fusion splicer. The input/output splice loss is ~1.5 dB, and the total insertion loss of HC-PCF filled with FGO is ~4.1 dB.

FGO used in our experiments was synthesized by arc-discharge method using a buffer gas containing carbon dioxide [22]. It can be well dispersed in common organic solvents. Based on an atomic force microscopy statistical height analysis, the distribution of FGO is mainly four to five layers with layer size of –100–300 nm [22]. GO is understood to be partially oxidized graphene. The saturable absorption in GO is attributed to the presence of pristine graphene nanoislands with sp^2-hybridized carbon atoms. Since the relative content of the nonoxygenated sp^2 carbon atoms in FGO is much higher than that in conventional GO using chemical methods, FGO has a faster energy relaxation of hot carriers and stronger saturable absorption than conventional GO. Fast carrier relaxation combined with well solution processing capability arises from the large fraction of sp^2 carbon atom inside the FGO sheet together with oxidation mainly existing at the edge areas [23]. FGO shows a broadband absorption in the whole spectral region as shown in Fig. 2(a).

FGO was dispersed in N,N-dimethylmethanamide (DMF) with concentration of 0.1 mg/ml and then was filled into the core of HC-PCF (HC1550-02, Crystal Fiber) through a selective hole filling process [24]. The insets of Fig. 1 are the cross section images of the HC-PCF before (right) and after (left) infiltration of FGO solution, observed by the use of a microscope (Nikon ECLIPSE 80i). The central hole is perfectly filled while the holes in the cladding are not filled. Figure 2(b) plots the measured transmission as a function of average pump power at the wavelength of 1550 nm (using a probe laser with the pulse width of 2 ps and the repetition rate of 20 GHz). At low input power level, the transmission is almost independent of pump power. However, the transmission increases by 8% due to absorption saturation when the incident average power is raised to 3.5 mW. The change of transmission (8%) is larger than that of graphene-polymer composite (1.3%)[11]. Moreover, FGO also presents a large saturable absorption at 800 nm [23].

Figure 3 summarizes the characteristics of the optical pulses emitted from the fiber laser mode locked by HC-PCF filled with FGO. The pulse train was measured by use of a high speed photo-detector (Newfocus 1414, 25 GHz), which could be connected with an oscilloscope (Tektronix, TPS 2024) or a Communications Signal

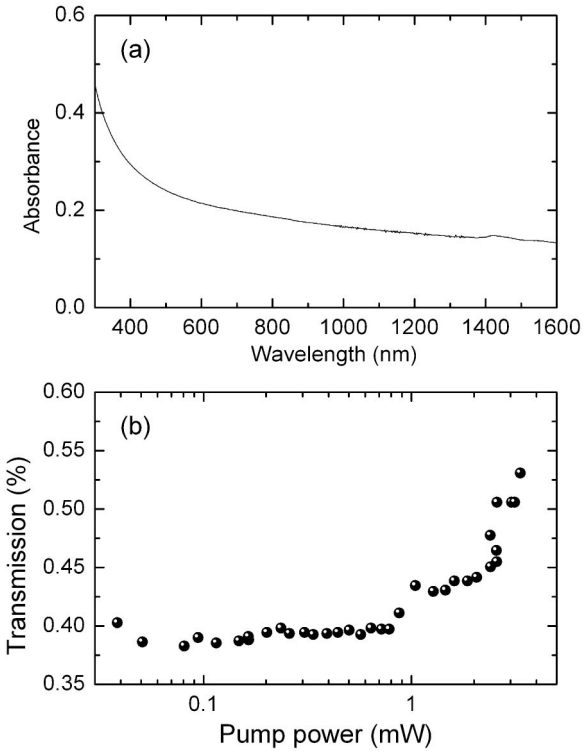

Fig. 2. (a) Absorption spectrum of FGO solution in DMF. (b) Typical transmission of the HC-PCF filled with FGO as a function of average pump power.

Analyzer (Tektronix CSA 803C). The laser optical spectrum was obtained by use of an optical spectrum analyzer (ANDO AQ6319) with 0.01 nm resolution. The pulse train of the laser output shown in Fig. 3(a) has a period of 131 ns, which matches well with the cavity round-trip time and verifies that the laser is mode locked. Figure 3(b) shows the optical spectrum of the mode-locked pulses. The spectral width of the pulses has the full width at half-maximum value of 0.11 nm and is centered at 1561.2 nm. Figure 3(c) demonstrates the pulse intensity profile, and the pulse width of 4.85 ns can be observed for a sech^2 curve fit. When the pump power is increased to ~38 mW, stable mode locking can be initiated by adjusting the PC. The laser output power versus the pump power is shown in Fig. 3(d). When the pump power is ~210 mW, the laser output power of ~4.3 mW with the pulse energy of ~0.56 nJ can be obtained. Such a long-pulse passive mode-locking regime has been recently identified by employing an SA [5,25–27].

To study the operation stability, we have measured the radio frequency (RF) spectrum of the passively mode-locked fiber laser by real-time spectrum analyzer (Tektronix RSA 3303A, 3 GHz). Its fundamental peak locates at the cavity repetition rate (7.68 MHz), as shown in Fig. 3(e), with the signal-to-noise ratio of 81 dB (10^8 contrast). Figure 3(f) reveals the RF spectrum measured around the tenth harmonic of the repetition rate at 76.8 MHz. The signal-to-noise ratio of >70 dB can also be observed, indicating good mode-locking stability [28].

In conclusion, we have demonstrated a nanosecond-pulse erbium-doped fiber laser that is passively mode locked by an HC-PCF filled with FGO solution. The flexibility offered by the graphene solution, along with the

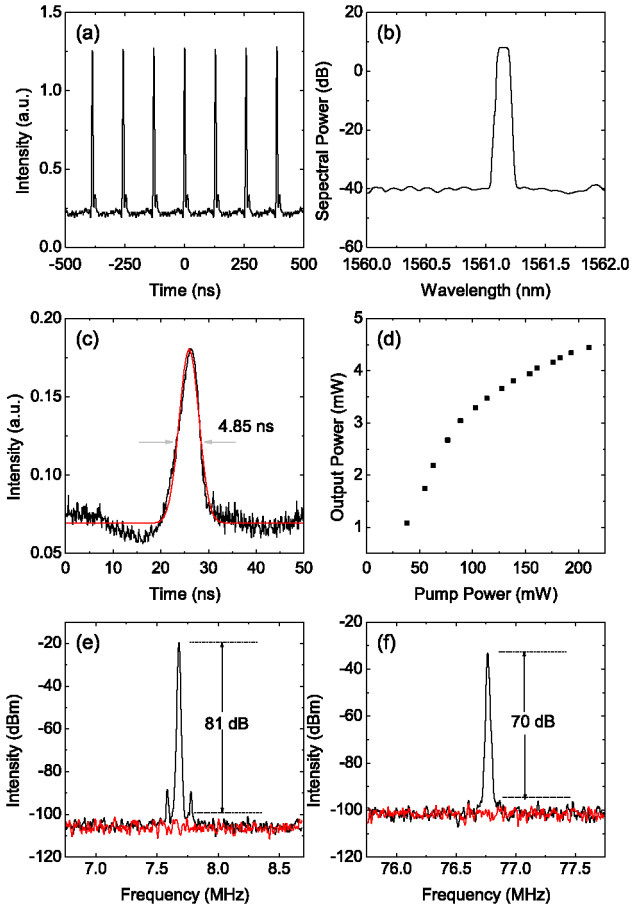

Fig. 3. (Color online) Characteristics of the mode-locked pulses. (a) Typical laser output pulse train. (b) Output pulse spectrum, centered at 1561.2 nm. (c) Pulse shape (black line) with sech^2 fit (red line). (d) Output power versus pump power. (e) RF spectrum measured around the fundamental repetition rate of 7.68 MHz. (f) RF spectrum measured around the tenth harmonic of the repletion rate at 76.8 MHz. The red traces in (e) and (f) depict the background when the laser is switched off.

HC-PCF, can lead to a simple and efficient approach to integrate the graphene into the optical system.

This work was supported by Hong Kong SAR government through a general research fund grant PolyU 5298/10E and the Hong Kong Polytechnic University research grant G-YX3R.

References

1. G. Steinmeyer, D. H. Sutter, L. Gallmann, N. Matuschek, and U. Keller, Science **286**, 1507 (1999).
2. O. Okhotnikov, A. Grudinin, and M. Pessa, New J. Phys. **6**, 177 (2004).
3. F. Wang, A. G. Rozhin, V. Scardaci, Z. Sun, F. Hennrich, I. H. White, W. I. Milne, and A. C. Ferrari, Nat. Nanotechnol. **3**, 738 (2008).
4. A. V. Tausenev, E. D. Obraztsova, A. S. Lobach, A. I. Chernov, V. I. Konov, P. G. Kryukov, A. V. Konyashchenko, and E. M. Dianov, Appl. Phys. Lett. **92**, 171113 (2008).
5. E. J. R. Kelleher, J. C. Travers, Z. Sun, A. G. Rozhin, A. C. Ferrari, S. V. Popov, and J. R. Taylor, Appl. Phys. Lett. **95**, 111108 (2009).
6. T. Hasan, Z. P. Sun, F. Q. Wang, F. Bonaccorso, P. H. Tan, A. G. Rozhin, and A. C. Ferrari, Adv. Mater. **21**, 3874 (2009).
7. R. R. Thomson, N. D. Psaila, Z. Sun, T. Hasan, A. G. Rozhin, A. C. Ferrari, and A. K. Kar, Appl. Phys. Lett. **97**, 111114 (2010).
8. A. Martinez, K. M. Zhou, I. Bennion, and S. Yamashita, Opt. Express **18**, 11008 (2010).
9. F. Shohda, M. Nakazawa, J. Mata, and J. Tsukamoto, Opt. Express **18**, 9712 (2010).
10. Q. L. Bao, H. Zhang, Y. Wang, Z. H. Ni, Y. L. Yan, Z. X. Shen, K. P. Loh, and D. Y. Tang, Adv. Funct. Mater. **19**, 3077 (2009).
11. Z. Sun, T. Hasan, F. Torrisi, D. Popa, G. Privitera, F. Wang, F. Bonaccorso, D. M. Basko, and A. C. Ferrari, ACS Nano **4**, 803 (2010).
12. H. Zhang, D. Y. Tang, R. J. Knize, L. M. Zhao, Q. L. Bao, and K. P. Loh, Appl. Phys. Lett. **96**, 111112 (2010).
13. D. Popa, Z. Sun, F. Torrisi, T. Hasan, F. Wang, A. C. Ferrari, Appl. Phys. Lett. **97**, 203106 (2010).
14. Y. W. Song, S. Y. Jang, W. S. Han, and M. K. Bae, Appl. Phys. Lett. **96**, 051122 (2010).
15. Q. Bao, H. Zhang, Z. Ni, Y. Wang, L. Polavarapu, Z. Shen, Q.-H. Xu, D. Tang, and K. Loh, Nano Res. **4**, 297 (2011).
16. Z. Sun, D. Popa, T. Hasan, F. Torrisi, F. Wang, E. J. R. Kelleher, J. C. Travers, and A. C. Ferrari, Nano Res. **3**, 653 (2010).
17. Q. L. Bao, H. Zhang, J. X. Yang, S. Wang, D. Y. Tong, R. Jose, S. Ramakrishna, C. T. Lim, and K. P. Loh, Adv. Funct. Mater. **20**, 782 (2010).
18. F. Bonaccorso, Z. Sun, T. Hasan, and A. C. Ferrari, Nat. Photonics **4**, 611 (2010).
19. K. P. Loh, Q. Bao, G. Eda, and M. Chhowalla, Nature Chem. **2**, 1015 (2010).
20. G. Eda and M. Chhowalla, Adv. Mater. **22**, 2392 (2010).
21. L. E. Nelson, D. J. Jones, K. Tamura, H. A. Haus, E. P. Ippen, Appl. Phys. B **65**, 277 (1997).
22. Y. P. Wu, B. Wang, Y. F. Ma, Y. Huang, N. Li, F. Zhang, and Y. S. Chen, Nano Res. **3**, 661 (2010).
23. X. Zhao, Z. B. Liu, W. B. Yan, Y. Wu, X. L. Zhang, Y. S. Chen, J. G. Tian, Appl. Phys. Lett. **98**, 121905 (2011).
24. L. Xiao, W. Jin, M. S. Demokan, H. L. Ho, Y. L. Hoo, and C. L. Zhao, Opt. Express **13**, 9014 (2005).
25. W. H. Renninger, A. Chong, and F. W. Wise, Opt. Lett. **33**, 3025 (2008).
26. S. Kobtsev, S. Kukarin, and Y. Fedotov, Opt. Express **16**, 21936 (2008).
27. X. Tian, M. Tang, P. P. Shum, Y. Gong, C. Lin, S. Fu, and T. Zhang, Opt. Lett. **34**, 1432 (2009).
28. D. Linde, Appl. Phys. B **39**, 201 (1986).